Available online at www.sciencedirect.com
ScienceDirect
Journal of the European Ceramic Society 29 (2009) 2153–2161
www.elsevier.com/locate/jeurceramsoc

# Effect of soaking time on phase composition and topography and surface microstructure in vitrocrystalline whiteware glazes

Linda Fröberg [a,*], Thomas Kronberg [b], Leena Hupa [a]

[a] *Process Chemistry Centre, Åbo Akademi University, Biskopsgatan 8, FI-20500 Turku, Finland*
[b] *Ido Bathroom Ltd., Sanitec Group, FI-10600 Ekenäs, Finland*

Received 4 September 2008; received in revised form 8 January 2009; accepted 14 January 2009
Available online 10 February 2009

**Abstract**

The effect of soaking period on the phase composition and topography of raw glazes was discussed. The work had two goals: (i) to establish the potential of manufacturing glazes with a desired surface structure from un-fritted formulations in a fast single cycle for tiles and (ii) to clarify the effects of shortening the firing time on the phase composition and surface roughness of traditionally fired products such as sanitaryware. The results can be applied to adjust the glaze composition for given firing cycles in order to improve the chemical resistance and to achieve the desired microstructure through controlled surface composition.


*Keywords:* Firing; Microsructure-final; Surfaces; Glaze

## 1. Introduction

During recent years the demands of shorter firing cycles and an easy control of surface microstructure have called for the use of fritted compositions. Raw glaze formulations have to a large extent, either entirely or partly, been replaced by fritted formulations in tile manufacturing. However, in the case of tiles fired at temperatures above 1200 °C for demanding environments where water impermeability, high mechanical strength, or frost resistance are required, e.g. outdoors and in baths and swimming pools, raw glazes are still a competitive alternative to fritted formulations. In sanitaryware industry, raw glazes are common, whereas the long soaking period gives a proper fusion of the raw materials. The elimination of the glaze melt fritting process leads to substantial savings in total energy consumption. Additionally, the accessibility to local raw materials is an important factor contributing to the use of raw glazes. This work was based on real case ceramic-tile and sanitaryware industries using mainly raw glazes in their production. For these industries, raw glazes are cost efficient alternatives, as many of the raw material minerals used come from local mining plants. Continuous utilization of raw glazes depends on whether the formulations can be adapted for future changes in glaze firing cycles and for modern needs of surface quality and properties.

Phase composition of glazes is usually controlled by the crystallization tendency of the glassy melt during cooling from the firing temperature. Crystalline phases developed in traditionally fired glazes have been found to correspond to those found in relevant phase diagrams, whereas the phases formed in shorter firing cycles depend on the first raw material reactions.[1,2] The crystalline phases formed in fast-firing reactions were found to be predominantly alkaline earth silicates, i.e. wollastonite, pseudowollastonite or diopside.[1,2] Especially the wollastonite-type crystals had poor chemical resistance in acidic to slightly alkaline environments.[3–6]

During recent years, much effort has gone into developing fritted formulations that nucleate and crystallize into glass-ceramic coatings. These coatings are reported to have better mechanical and chemical properties than the traditional partly crystalline glazes.[7–11] Crystallization mechanisms and phase formation in parent glasses within, e.g. the quaternary $SiO_2$–$Al_2O_3$–CaO–MgO as well as the ternaries CaO–MgO–$SiO_2$, $Al_2O_3$–CaO–MgO and $Li_2O$–$Al_2O_3$–$SiO_2$, leading to crystallization in the primary fields of cordierite,

* Corresponding author. Tel.: +358 2 215 4563; fax: +358 2 215 4962.
*E-mail address:* lfroberg@abo.fi (L. Fröberg).

0955-2219/$ – see front matter © 2009 Elsevier Ltd. All rights reserved.
doi:10.1016/j.jeurceramsoc.2009.01.012

Table 1
Raw material composition of the experimental glazes (wt%).

| Glaze | Kaolin | Feldspar | Dolomite | Limestone | Corundum | Quartz |
|---|---|---|---|---|---|---|
| 1 | 6.0 | 74.6 | 14.5 | 0.0 | 0.0 | 4.9 |
| 2 | 8.0 | 26.0 | 15.0 | 17.8 | 13.0 | 20.2 |
| 3 | 8.0 | 26.2 | 15.0 | 17.7 | 0.3 | 32.8 |
| 4 | 5.0 | 42.5 | 14.5 | 17.0 | 0.0 | 21.0 |
| 5 | 5.0 | 27.7 | 0.0 | 27.0 | 1.4 | 38.9 |
| 6 | 5.5 | 25.9 | 0.0 | 43.0 | 0.9 | 24.7 |
| 7 | 5.0 | 26.9 | 7.5 | 22.6 | 14.3 | 23.7 |
| 8 | 5.0 | 52.9 | 8.4 | 2.9 | 11.6 | 19.3 |
| 9 | 5.0 | 43.0 | 0.0 | 41.5 | 0.0 | 10.5 |
| 10 | 5.0 | 78.0 | 0.0 | 7.5 | 7.6 | 2.0 |
| 11 | 8.0 | 48.0 | 7.4 | 22.1 | 3.0 | 11.6 |
| 12 | 8.0 | 27.2 | 15.4 | 0.0 | 0.6 | 48.8 |
| 13 | 5.0 | 45.5 | 0.0 | 42.8 | 3.7 | 3.1 |
| 14 | 5.0 | 72.8 | 15.0 | 0.0 | 7.2 | 0.0 |
| 15 | 5.0 | 76.6 | 8.4 | 2.5 | 7.4 | 0.0 |

diopside, anorthite, mullite, gehlenite, wollastonite, and pseudowollastonite have been extensively studied.[10,12–15]

In the beginning of the 20th century, quite a few reports were addressed to the topics of improving the surface appearance of raw (un-fritted) lead glazes by adjusting the raw material composition. Much effort was put in finding satisfactory formulas for raw, good quality matt glazes, and alumina was suggested by many authors as a key factor for causing mattness.[16–21] A matted surface finish was reported to be a function of temperature as well as composition.[22] Anorthite, wollastonite, and tridymite were the main crystalline phases present in raw lead matt glazes showing a good quality matt appearance when fired at cones 03, 2, 4, and 6.[21] Despite the drastic changes in firing technology during the past decades, to our knowledge, only little attention has been paid to phase formation in raw leadless glazes as a function of firing parameters.

The raw material composition for un-fritted matt glazes needs to be carefully selected in order to ensure a completing of the reactions during firing, and further, to achieve the desirable crystallization giving the desired surface appearance. Nevertheless, the final phase composition depends not only on the raw material and oxide compositions, but also on the firing conditions. In addition, for a given firing cycle microstructure and durability of the surface should be taken as the key properties in selecting the glaze composition. The increased demands for the ware in service, such as cleanability and soil repellence, have due to latest requirements turned out to be highly valued properties for the performance of surfaces. Topographic characterization has become a common way to describe the surface properties, e.g. when estimating the soil attachment and cleanability of surfaces. According to our previous studies, cleanability was decreased by partial corrosion of the surface, i.e. due to leaching of wollastonite type of crystals. However, the overall cleanability depend on the surface roughness rather than on the phase composition.[23,24]

The goal of this work was to establish the changes in phase composition and topography of raw glazes within the compositional field for tiles and sanitaryware when firing cycle varied from fast to traditional. The focus was on evolving the knowledge in phase development, rather than on developing commercially attractive compositions. Understanding the phase development during firing gives tools for choosing the composition which gives a desired surface morphology. This paves the road for better glaze quality in terms of, e.g. chemical resistance, soiling and cleaning properties.

## 2. Materials and methods

Fifteen experimental glazes were ball milled from commercial-grade raw materials, and applied on green floor tiles in a waterfall process, i.e. the method commonly used in tile manufacture. The laboratory scale coating line gave a reproducible and even layer. The compositions of the experimental glazes were statistically chosen and covered the range of interest for ceramics fired at about 1200–1250 °C (cf. Tables 1 and 2). The mineralogical compositions of the raw materials were obtained from the raw material producers. The variations in compositions were taken into consideration when calculating the oxide composition for the experimental glazes. The experimental compositions were designed to reveal the development and

Table 2
Oxide composition of the experimental glazes (wt%).

| Glaze | $Na_2O$ | $K_2O$ | MgO | CaO | $Al_2O_3$ | $SiO_2$ |
|---|---|---|---|---|---|---|
| 1 | 4.6 ± 0.4 | 5.4 ± 0.4 | 3.5 ± 0.1 | 5.6 ± 0.2 | 17.5 ± 0.1 | 63.5 ± 0.9 |
| 2 | 1.8 ± 0.2 | 2.2 ± 0.2 | 4.0 ± 0.1 | 17.5 ± 0.3 | 25.0 ± 0.3 | 49.5 ± 0.4 |
| 3 | 1.8 ± 0.2 | 2.3 ± 0.2 | 4.0 ± 0.1 | 17.4 ± 0.3 | 10.1 ± 0.0 | 64.5 ± 0.7 |
| 4 | 2.8 ± 0.3 | 3.4 ± 0.3 | 3.8 ± 0.0 | 16.8 ± 0.2 | 11.7 ± 0.0 | 61.4 ± 0.8 |
| 5 | 1.8 ± 0.2 | 2.3 ± 0.2 | 0.1 ± 0.1 | 17.4 ± 0.4 | 10.0 ± 0.0 | 68.4 ± 0.8 |
| 6 | 1.8 ± 0.2 | 2.3 ± 0.2 | 0.2 ± 0.2 | 29.9 ± 0.4 | 10.0 ± 0.1 | 55.9 ± 0.9 |
| 7 | 1.8 ± 0.2 | 2.2 ± 0.2 | 2.0 ± 0.1 | 17.6 ± 0.3 | 24.9 ± 0.3 | 51.5 ± 0.5 |
| 8 | 3.2 ± 0.3 | 3.8 ± 0.3 | 2.0 ± 0.0 | 5.0 ± 0.2 | 25.0 ± 0.2 | 61.1 ± 0.6 |
| 9 | 3.0 ± 0.3 | 3.6 ± 0.3 | 0.2 ± 0.2 | 28.9 ± 0.3 | 12.3 ± 0.1 | 52.1 ± 0.9 |
| 10 | 4.6 ± 0.4 | 5.4 ± 0.4 | 0.0 ± 0.0 | 5.1 ± 0.3 | 25.0 ± 0.3 | 59.9 ± 0.8 |
| 11 | 3.2 ± 0.3 | 3.8 ± 0.3 | 2.0 ± 0.1 | 17.5 ± 0.3 | 17.5 ± 0.2 | 56.0 ± 0.8 |
| 12 | 1.7 ± 0.2 | 2.2 ± 0.2 | 3.7 ± 0.0 | 5.4 ± 0.1 | 9.9 ± 0.0 | 77.1 ± 0.5 |
| 13 | 3.2 ± 0.3 | 3.8 ± 0.3 | 0.2 ± 0.2 | 30.0 ± 0.3 | 17.5 ± 0.3 | 45.4 ± 0.8 |
| 14 | 4.5 ± 0.4 | 5.2 ± 0.4 | 3.6 ± 0.1 | 5.8 ± 0.2 | 24.5 ± 0.3 | 56.4 ± 0.7 |
| 15 | 4.6 ± 0.4 | 5.4 ± 0.4 | 2.0 ± 0.0 | 5.0 ± 0.2 | 25.0 ± 0.3 | 58.0 ± 0.7 |

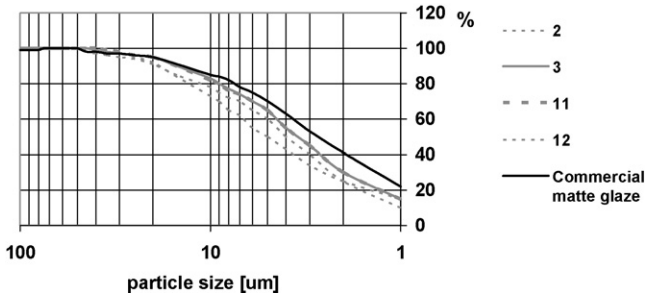


Fig. 1. Grain size distribution of four experimental glazes and a commercial matt glaze.

crystallization of different phases rather than to give glazes for commercial applications. Neither opacifying agents nor heavy metals such as barium oxide and zinc oxide were added to the batches. The feldspar used consisted of equal amounts of orthoclase and albite. Thus, the formation of typical crystals based on sodium, potassium, magnesium, calcium as well as aluminum and silicon oxides were considered.

The oxide compositions in Table 2 suggest that wollastonite crystals would be formed in compositions high in lime, but low in alumina and magnesia (glazes 5, 6, and 9). Correspondingly high magnesia content suggest for diopside formation (glazes 2, 3, 4, and 12). The other glazes are high in alumina thus favoring the formation of plagioclase type of crystals.

The milling time for the experimental glazes was adjusted to 20 min for each 500 g batch in order to obtain the grain size distribution corresponding to a commercial matt glaze. Fig. 1 shows the grain size distribution of four experimental glazes and a commercial matt glaze.

Glazed tiles were fired both industrially in a roller kiln and in a laboratory furnace (carbolite RHF 16/35). For the industrial firing, a typical fast-firing cycle for traditional single fired glazes was applied. The firing cycle of roughly 1 h included a 20 min heating ramp to 1215 °C, a 2–5 min soaking time at this temperature, and cooling down to room temperature. Firing in laboratory scale was carried out according to four different cycles. The heating rate (21.6 °C/min) and the cooling rate (4.6 °C/min) were equal for each firing cycle, but the soaking period varied. In the shortest firing cycle the top temperature was only reached, after which cooling took place. The other three firing cycles included 1, 4, and 24 h soaking. The top temperature in each firing cycle was 1215 °C.

## 3. Results and discussion

### 3.1. Phase composition

The phase composition was found to be sensitive to both glaze composition and firing time. Glazes ranging from highly glossy to highly matt were produced. Mattness was mainly caused by devitrification, but in some glazes un-maturity gave rise to a semi-matt or matt surface. The number, size, and composition of the crystals formed in the glazes varied. The main crystalline phases in the surfaces after each firing were identified by X-ray diffraction (X'pert by Philips, Cu Kα radiation) and scanning electron microscopy equipped for electron dispersive X-ray analysis (FEG-SEM, LEO 1530 from Zeiss/EDXA from Vantage by Thermo Electron Corporation), cf. Table 3. SEM images of glazes 2, 5, and 11 after different firing cycles are given in Fig. 2.

Table 3
Main crystalline phases identified in the glazes after each firing cycle by X-ray diffraction and SEM-EDX analyses. D, diopside; W, wollastonite; PW, pseudowollastonite; Q, quartz; An, anorthite; Al, albite. The dominating phase in the plagioclase solid solution is underlined.

| Glaze | Industrial fast-firing | Soaking time at top temperature 1215 °C | | | |
|---|---|---|---|---|---|
| | | 0 h | 1 h | 4 h | 24 h |
| 1 | D | D + Al | (Q) | (Q) | (Q) |
| 2 | D | D + An | An | An | An |
| 3 | D + W | D + W | D | D | D |
| 4 | D + W | D + W | D | D | (Q) |
| 5 | PW | PW | PW | PW | PW |
| 6 | PW | PW + An | PW + An | PW + An | (Q) |
| 7 | W | W | An | An | An |
| 8 | D | D + An − Al | D + An − Al | An − Al | An − (Al) |
| 9 | PW | PW | PW + An | PW + An | PW + An |
| 10 | W | W + An − Al | W + An − Al | An − Al | An − (Al) |
| 11 | W | W | An | An | An |
| 12 | D | D | D | D | D |
| 13 | PW | PW | PW + An | PW + An | PW + An |
| 14 | D | D + An − Al | An − Al | An − Al | An − Al |
| 15 | D | D + An − Al | An − Al | An − Al | An − Al |

#### 3.1.1. Industrial- and laboratory scale fast-firing

After the industrial fast-firing, all glazes contained wollastonite (β-$CaO{\cdot}SiO_2$), pseudowollastonite (α-$CaO{\cdot}SiO_2$), or diopside ($CaO{\cdot}MgO{\cdot}2SiO_2$). Occasionally residual crystals of un-reacted quartz and corundum were found. The feldspar-rich glazes with low content of alkaline earths were glossy, while decreased feldspar and increased alkaline earths gave matt surfaces. In the glossy glazes only tiny wollastonite or diopside crystals were identified together with residual quartz and corundum.

The same crystals as in the industrial fast-firing were also observed after the shortest laboratory scale firing including no soaking. However, after this firing cycle also plagioclase (i.e. anorthite–albite solid solution) was observed in the alumina-rich glazes (glazes 2, 7, 8, 10, 14, and 15). The slower heating and cooling rates in the laboratory scale furnace in comparison to the industrial fast-firing cycle were assumed to allow the crystallization of plagioclase and also to enhance the crystal growth, cf. Fig. 2.

Crystal formation in both the industrial- and laboratory scale fast-firing cycles was assumed to strongly depend on the starting raw material mixture. Within the $CaO–MgO–SiO_2$ equilibrium system, pseudowollastonite, diopside and silicon dioxide are formed through crystallization of the melt at the ternary eutectic 1320 °C. Thus, in the glazes fired to 1215 °C the crystalline phases obtained after the shortest firing cycles cannot be formed through crystallization from the melt. Instead crystallization was

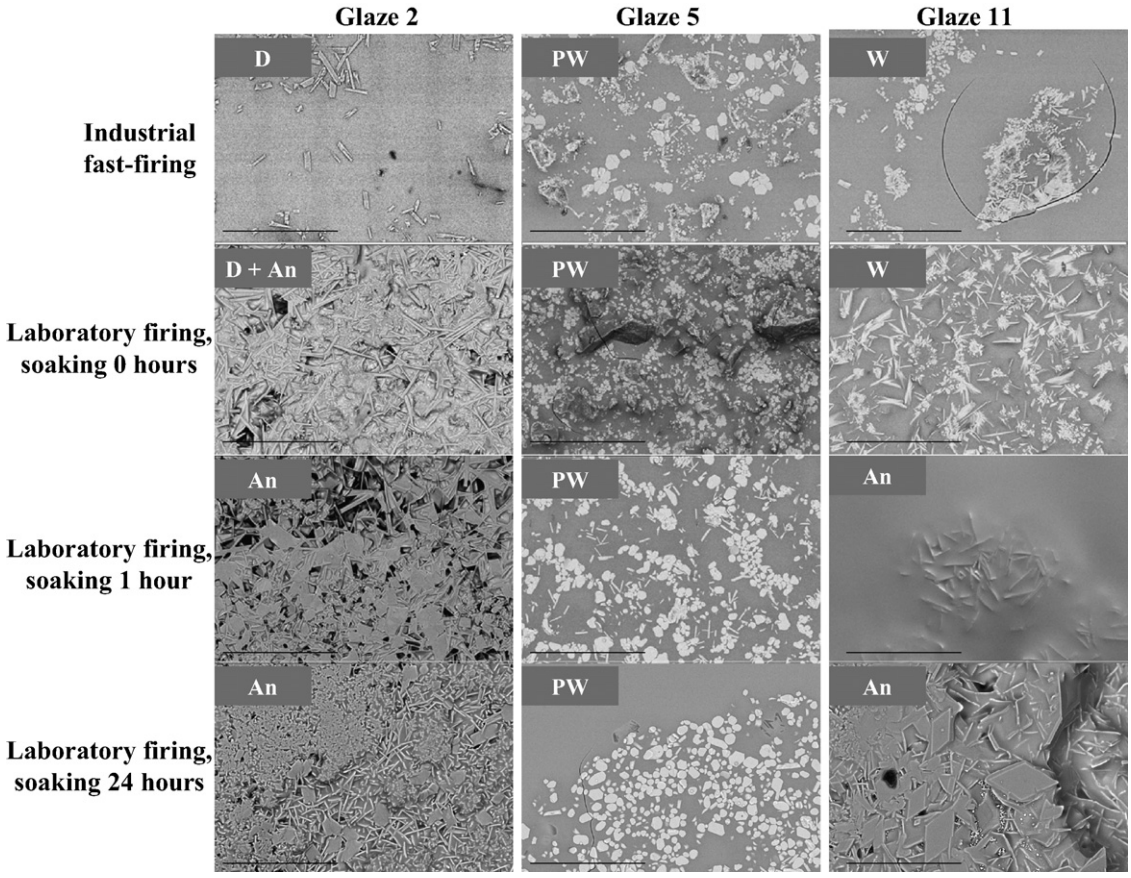


Fig. 2. SEM images of glazes 2, 5, and 11 when fast-fired industrially and in laboratory scale according to the cycles with 0, 1, and 24 h soaking. The main crystalline phases identified by SEM-EDX and XRD analysis are labeled. D, diopside; W, wollastonite; PW, pseudowollastonite; An, anorthite. The bar equals to 100 μm.

suggested to occur through raw material reactions between, e.g. quartz and limestone or dolomite whereas wollastonite, pseudowollastonite and diopside were formed.

In lime-rich magnesia-free glazes, pseudowollastonite was identified as the main crystal type after the shortest firing cycles. With longer firing cycles, pseudowollastonite gradually melted if not enough alumina was present for anorthite formation. In SEM and COM (confocal optical microscopy) images the pseudowollastonite crystals showed a typical hexagonal plate-like structure.[25–27] Also X-ray analysis suggested pseudowollastonite which was supported by the roughly 1:1 ratio of calcium to silicon according to EDX-analysis. In magnesia containing lime-rich glazes, pseudowollastonite was not formed. Instead, needle and feather-like wollastonite crystals were seen in SEM micrographs. Finally, diopside was identified if magnesia content was higher than 2 wt%. In alkali–lime–silica glasses, 4 wt% MgO has been reported to bring about diopside formation as the primary phase rather than wollastonite.[28]

In lime-rich glazes with high magnesia content, feather-like wollastonite as well as diopside was present in the same glaze when fast-firing industrially or according to the shortest firing cycle in laboratory scale. In longer firing cycles wollastonite dissolved, leaving diopside as the sole phase (glazes 3 and 4). Where the alumina content was high enough, diopside and wollastonite crystals initially formed were transformed with longer firing to anorthite (glazes 2 and 7). The length and the shape of the diopside crystals varied with firing cycle and composition. In the industrially fired glazes, 2–10 μm long, plate-like crystals were common, while diopside formed in the laboratory scale firings were 10–40 μm long with a needle-like structure.

### 3.1.2. *Laboratory scale firing; 1–24 h soaking*

In the longer firing cycles, wollastonite, pseudowollastonite, and diopside gradually dissolved and contributed to the formation of plagioclase, i.e. a solid solution of anorthite–albite. Overall, anorthite ($CaO^{\bullet}Al_2O_3{}^{\bullet}2SiO_2$) and albite ($Na_2O^{\bullet}Al_2O_3{}^{\bullet}6SiO_2$) were the main crystals identified in the longer firing cycles. No plagioclase-type crystals were formed in glazes low in feldspar and corundum and with a low to moderate lime content (glazes 3, 4, 5, and 12). In these glazes wollastonite, pseudowollastonite and diopside were the predominant crystal forms as in the shorter firing cycles. The amount of glassy phase in these glazes increased with increasing soaking time as the primarily formed crystals dissolved.

Crystal formation in the longer firings included alumina, whereby, e.g. the systems $CaO–Al_2O_3–SiO_2$, $Na_2O–Al_2O_3–SiO_2$, and $K_2O–Al_2O_3–SiO_2$ were of interest. In the $CaO–Al_2O_3–SiO_2$ system the compatibility triangle pseudowollastonite–anorthite–silicon dioxide has the lowest melting temperature with the ternary eutectic at 1170 °C. The alkaline oxides were, however, likely to further decrease

this melt formation temperature. The ternary eutectic gives pseudowollastonite, anorthite and silicon dioxide as possible phases in the glazes. For the sodium and potassium systems also albite, mullite, or potassium feldspar are likely, while they are present at eutectics below the top firing temperature for the experimental glazes (1215 °C).

Anorthite was the dominating phase when fired in the longest firing cycle. Anorthite has been reported to consist of a network of lath-like crystals with interlocking grain boundaries, and further, to form from wollastonite during firing if alumina is present in the composition.[25,27,29] In this work alumina was also found to be important for plagioclase formation. Accordingly, no plagioclase was observed in the alkaline feldspar-rich glaze containing no additional corundum. Instead this glaze formed a glossy surface.

Three different routes of plagioclase formation depending on composition could be distinguished. Firstly, in feldspar-rich glazes containing corundum, anorthite–albite solid solution with needle-like network structure was formed (cf. Fig. 3). With prolonged soaking the plagioclase composition was shifted towards anorthite. Secondly, in glazes with low feldspar, *anorthite* was suggested to form by the reactions between quartz, corundum, and limestone. After 1 h soaking, the glazes were more or less covered with a network of rectangular flakes, which were identified to anorthite by X-ray analysis. At longer soaking also needle-like crystals were present. According to EDX-analysis some magnesia was present in the needles, but X-ray analysis gave anorthite as the only crystalline phase. A third route to anorthite was suggested through partial dissolution of wollastonite or pseudowollastonite into the feldspar-rich melt in glazes with intermediate feldspar, but high lime content. Anorthite crystals then developed in the melt. Already after 1 h's soaking some anorthite was observed, and after the longest soaking time rhombic anorthite crystals were identified (cf. Fig. 3).

### 3.2. Topography vs. phase composition

The predominant phases in the glazes after each firing cycle are summarized in the simplified ternary phase diagrams $Al_2O_3$–$SiO_2$–$MO + M_2O$ of Fig. 4. The total sum of alkaline and alkaline earth oxides ($Na_2O$, $K_2O$, CaO, and MgO) is given by $MO + M_2O$. The diagrams do not, however, give the size and relative amount of crystals. Only the phases observed by X-ray analysis are indicated.

The diagram shows that the wollastonite, pseudowollastonite and diopside crystals in the alumina-rich glazes were transformed into anorthite–albite, i.e. plagioclase, with prolonged soaking. If the alumina and total alkaline and alkaline earth contents were low, however, wollastonite, pseudowollastonite and diopside were also found after the longest soaking. Higher contents of alkalis and alkaline earths, in turn promoted the formation of plagioclase.

The size and amount of the crystals in the glazes, and thus the surface topography, varied with composition and firing cycle. Whitelight confocal microscopy (COM, NanoFocus μsurf®) was used to capture 3D images of the glaze surfaces and to measure surface roughness values. Surface roughness was also measured for one matt and one glossy commercial floor-tile glaze manufactured under the same conditions in the industrial kiln as the experimental glazes. Whitelight COM has recently been developed for measuring surface topography of industrial and optically complex surface structures with high vertical and lateral resolution. This rapid and nondestructive method is especially suitable for ceramics with variable surface topography. In this work, the average 3D surface roughness (Sa) according to DIN EN ISO 4287 was measured with a 100× objective lens giving a vertical resolution of 2–5 nm and numerical aperture 0.8–0.95 for a measurement field of 160 μm × 154 μm. For this resolution, the cut-off wavelength 80 μm was applied. The average surface roughness varied from 0.01 to 8.1 μm depending on firing cycle and glaze composition.

#### 3.2.1. Influence of soaking time on surface roughness

The standard deviation for Sa was obtained by measuring six areas on each surface. Highest roughness values were measured for the un-mature surfaces in the industrial fast-firing. The surface roughness also increased with anorthite formation. Glazes could be classified into three groups according to the trends in the surface roughness with soaking period:

(i) Glazes in which diopside, wollastonite, or pseudowollastonite was the main crystal type in all firing cycles (A in Fig. 5).
(ii) Glazes that after fast-firing contained mainly diopside, wollastonite, or pseudowollastonite but also some plagioclase, whereas after prolonged firing only plagioclase was present (B in Fig. 5).
(iii) Glazes that after the fast-firing, contained mainly diopside, wollastonite, or pseudowollastonite, and exhibited a continuous growth, mostly of anorthite, as firing continued (C in Fig. 5).

Group (i) glazes contained abundant crystals in the surface after the fast-firing cycle, but during longer soaking times the crystals partly, or completely, melted and the surface became smoother and glossier. Thus, the average roughness of these glazes decreased with soaking time (Fig. 5). The average roughness of glazes in group (ii) was mostly relatively high, but smoothening was evident when soaking was 1 h. At longer soaking, wollastonite, pseudowollastonite and diopside dissolved. The dissolved alkaline earths contributed to the formation of plagioclase crystals. At the longest soaking periods (4 and 24 h) the plagioclase crystals grew in size, leading to increased surface roughness (Fig. 5). The third group of glazes showed a continuous growth of crystals as is reflected in the roughness values (Fig. 5). The high corundum content favored the growth of large anorthite crystals.

The 3D COM images in Fig. 6 show typical microstructure and topography as a function of soaking period, for one glaze in each group A–C. The crystalline phases according to the X-ray analysis are indicated together with the average roughness (Sa) value for each surface. Their values as a function of soaking time correlated with the overall appearance of the surfaces.

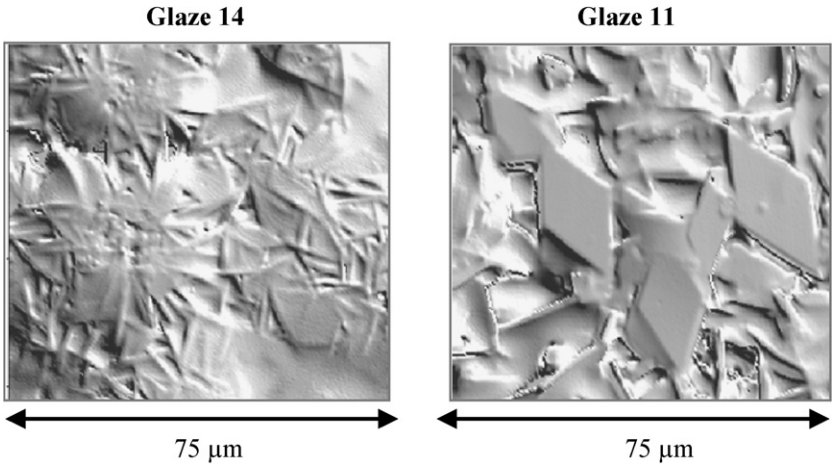


Fig. 3. COM image of anorthite–albite crystals with needle-like network structure in feldspar-rich compositions (Glaze 14), and rhombic anorthite crystals in lime-rich compositions containing moderate amounts of feldspar (glaze 11). Both glazes were fired according to the longest firing cycle.

### 3.3. Matt vs. glossy surface finish

The results clearly indicate that short firing cycles gave intermediate phases, i.e. wollastonite, pseudowollastonite, or diopside, representing the first raw material reactions. However, the glazes fired at longer cycles can be assumed to react according to equilibrium reactions. According to Kingery et al., anorthite is the main crystalline phase in traditional glazes.[30] Also in this work, anorthite type of crystals were observed in the longer firing cycles in corundum containing glazes. If corun-

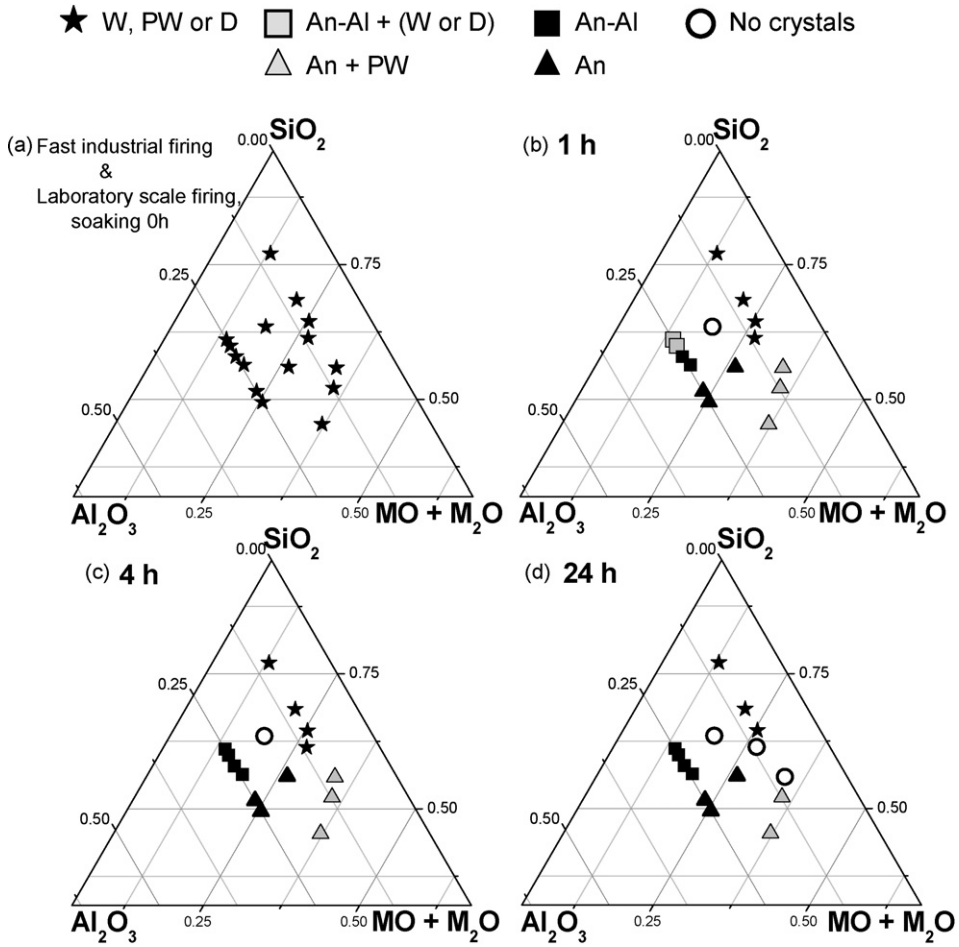


Fig. 4. Glaze composition (wt%) and crystalline phases of the experimental glazes according to XRD and SEM/EDXA. (a) industrial fast-firing and laboratory scale firing including no soaking. Laboratory scale firing soaking (b) 1 h, (c) 4 h, and (d) 24 h. $M_2O + MO = Na_2O + K_2O + MgO + CaO$. W, wollastonite; PW, pseudowollastonite; D, diopside; An-Al, anorthite–albite.

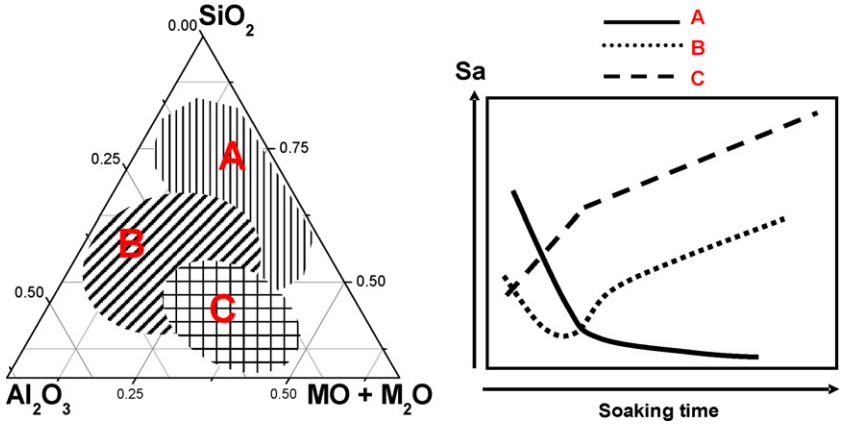


Fig. 5. Reduced ternary compositions showing areas (left), for trends in surface roughness (right) as a function of soaking time. Compositions rich in silica (A), alumina (B), alkali and alkaline earths (C).

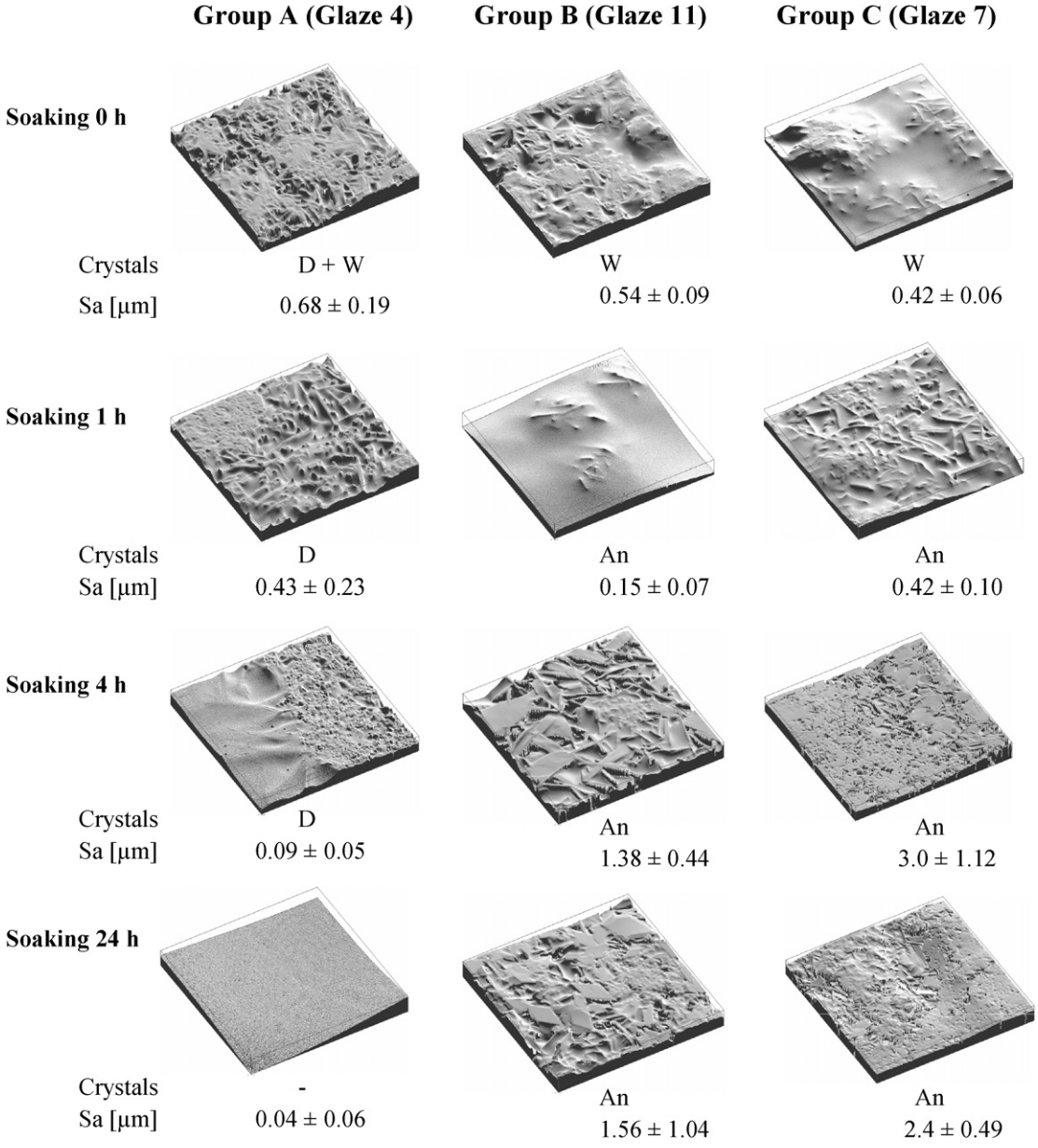


Fig. 6. COM images of glazes typical for groups A–C. The main crystalline phases in the surfaces and the roughness values for the surfaces, Sa (μm), are indicated. Image size: 160 μm × 158 μm.

dum was not present, anorthite type of crystals did not form. Instead, diopside or pseudowollastonite remained as the main crystal types. These crystals dissolved with increasing soaking. In all firing cycles, the degree of mattness could be adjusted by adjusting the glaze composition.

In industrial fast-firing of raw glazes, glossy surfaces were obtained only when the feldspar content was high. A matted surface finish was achieved through crystallization of wollastonite, pseudowollastonite, or diopside. Wollastonite crystals are known to have insufficient chemical resistance and should thus be avoided. Diopside gave, however, good quality matt glazes with tiny diopside crystals uniformly distributed in the surface. In compositions containing both dolomite and limestone, wollastonite formation was totally inhibited when the ratio corundum to silica was high. In these glazes anorthite was formed with longer soaking.

In traditional firing, glossy surfaces were achieved only in corundum-free compositions. If carbonate containing raw materials were present, diopside, wollastonite or pseudowollastonite was formed in the shorter cycles, giving the surface a matt appearance. By increasing the soaking time, mattness was reduced as the crystals dissolved. Higher feldspar contents shortened the soaking time required for achieving glossy surfaces. Again, wollastonite type of crystals was avoided by using some dolomite.

Traditional firing of corundum containing glazes allowed plagioclase types of crystals to form already after 1 h's soaking. Wollastonite, pseudowollastonite or diopside contributed to plagioclase formation as they gradually dissolved. Partial dissolution of wollastonite and quartz has been reported to support anorthite formation at temperatures above 1050 °C in ceramic mixtures for tiles.[27] Overall, wollastonite was observed only when firing in the shortest firing cycle, but pseudowollastonite remained in longer firings also. High feldspar glazes gave matt surfaces after the longest soaking time. In these glazes needle-like anorthite–albite crystals were formed. If soaking time was shortened, mattness was reduced. Intermediate or low feldspar glazes gave highly matted surfaces already after 1 h soaking. In these glazes anorthite formation was extensive, and mattness increased with increasing soaking.

## 4. Conclusions

Phase composition and topography of raw glazes changed with firing cycle. In short firing the surface morphology depended on initial raw material reactions and melt formation. At prolonged firing the surface morphology was controlled by the total oxide composition and equilibrium phase conditions at high temperatures.

In fast-firing glossy and smooth glazes were obtained when the feldspar content was high. Mattness was caused by crystallization of diopside, wollastonite and pseudowollastonite. These crystals were formed in initial raw material reactions in fast-firing cycles where the peak firing temperature was only just reached. Highest roughness values were observed for glazes with pseudowollastonite and residual quartz or corundum. Dolomite glazes had surface roughness values corresponding to commercial matt glazes. Thus, the problems with poor chemical durability due to wollastonite matts could be avoided by a high content of dolomite in the raw glaze.

At prolonged firing the phase development could be related with the corundum content. In corundum-free compositions glossy glazes were formed when the initially formed crystals gradually melted. Thus, the surface roughness of these glazes decreased with increasing soaking. In compositions that contained corundum, longer soaking times lead to plagioclase formation. Lime-rich compositions and long soaking gave rough surfaces due to extensive anorthite formation. The feldspar-rich compositions crystallized into anorthite–albite with prolonged soaking time. Thus, the high corundum content was assumed to aid crystallization of anorthite–albite. The results indicated that soaking time of traditionally fired raw glazes can be shortened if the total glaze composition is adjusted to retain a desired surface morphology and properties.

## Acknowledgments

This work is part of the Activities of the Åbo Akademi Process Chemistry Centre funded by the Academy of Finland in their Centres of Excellence Program. Funding has been provided by the Clean Surfaces 2002–2006 Technology Programme run by the Finnish Funding Agency for Technology and Innovation (Tekes), the Graduate School of Materials Research and Ido Bathroom Ltd.

## References

1. Fröberg, L., Kronberg, T., Hupa, L. and Hupa, M., Influence of firing parameters on phase composition of raw glazes. *J. Eur. Ceram. Soc.*, 2007, **27**, 1671–1675.
2. Fröberg, L., Vane-Tempest, S. and Hupa, L., Surface composition and topography of fast-fired raw glazes. In *Proceedings of the VIII World Congress on ceramic tile quality 1*, 2004, P.GI-143.
3. Fröberg, L., Kronberg, T., Törnblom, S. and Hupa, L., Chemical durability of glazed surfaces. *J. Eur. Ceram. Soc.*, 2007, **27**, 1811–1816.
4. Kronberg, T., Hupa, L. and Fröberg, K., Durability of mat glazes in hydrochloric acid solution. *Key Eng. Mater.*, 2004, **264–268**, 1565–1568.
5. Abdel-Hameed, S. A. M. and El-Kheshen, A. A., Thermal and chemical properties of diopside-wollastonite glass-ceramics in the $SiO_2$–CaO–MgO system from raw materials. *Ceram. Int.*, 2003, **29**, 265–269.
6. Bolelli, G., Cannilo, V., Lusvarghi, L., Manfredini, T., Siligardi, C., Bartuli, C. *et al.*, Plasma-sprayed glass-ceramic coatings on ceramic tiles: microstructure, chemical resistance and mechanical properties. *J. Eur. Ceram. Soc.*, 2005, **25**, 1835–1853.
7. Baldi, G., Generali, E., Leonelli, C., Manfredini, T., Pellacani, G. C. and Siligardi, C., Effects of nucleating agents on diopside crystallization in new glass-ceramics for tile glaze application. *J. Mater. Sci.*, 1995, **30**, 3251–3255.
8. Ferrari, A. M., Barbieri, L., Leonelli, C., Manfredini, T., Siligardi, C. and Bonamartini, A., Feasibility of using cordierite glass-ceramics as tile glazes. *J. Am. Ceram. Soc.*, 1997, **80**(7), 1757–1766.
9. Torres, F. J. and Alarcon, J., Microstructural evaluation in fast-heated cordierite-based glass-ceramic glazes for ceramic tile. *J. Am. Ceram. Soc.*, 2004, **87**, 1227–1232.
10. Yeketa, B. E., Alizadeh, P. and Rezazadeh, L., Floor tile glass-ceramic glaze for improvement of glaze surface properties. *J. Eur. Ceram. Soc.*, 2006, **26**, 3809–3812.
11. Leonelli, C., Manfredini, T., Paganelli, M., Pozzi, P. and Pellacani, G. C., Crystallization of some anorthite-diopside glass precursors. *J. Mater. Sci.*, 1991, **26**, 5041–5046.

12. Marhgussian, V. K. and Alizadeh, P., Effect of nucleating agents on the crystallization behavior and microstructure of $SiO_2$–CaO–MgO ($Na_2O$) glass-ceramics. *J. Eur. Ceram. Soc.*, 2000, **20**, 775–782.
13. Torres, F. J. and Alarcon, J., Pyroxene-based glass-ceramics as glazes for floor tiles. *J. Eur. Ceram. Soc.*, 2005, **25**, 349–355.
14. Leonelli, C., Manfredini, T., Paganelli, M., Pellacani, J. L., Amoros, J. L., Navarro, J. E. *et al.*, $Li_2O$–$SiO_2$–$Al_2O_3$–MeO glass-ceramics systems for tile glaze application. *J. Am. Ceram. Soc.*, 1991, **74**, 983–987.
15. Rincon, J. Ma., Romero, M., Marco, J. and Caballer, V., Some aspects of crystallization microstructure on new glass-ceramic glazes. *Mater. Res. Bull.*, 1998, **33**, 1159–1164.
16. Binns, C. F., The development of mat glazes. *Trans. Am. Ceram. Soc.*, 1903, **5**, 50.
17. Worcester, W. G., The function of alumina in a crystalline glaze. *Trans. Am. Ceram. Soc.*, 1908, **10**, 450.
18. Purdy, R. C., Mat glazes. *Trans. Am. Ceram. Soc.*, 1912, **14**, 671.
19. Forrest, K. P., A theory of the cause of mattness in glazes. *Trans. Am. Ceram. Soc.*, 1912, **14**, 682–690.
20. Staley, H. F., The microscopic examination of twelve matt glazes. *Trans. Am. Ceram. Soc.*, 1912, **14**, 691–709.
21. Parmalee, C. W. and Horak, W., The microstructure of some raw lead mat glazes. *J. Am. Ceram. Soc.*, 1934, **17**, 67–72.
22. Whitford, W. G., A study of three component normative systems in raw lead glazes. *Trans. Am. Ceram. Soc.*, 1917, **19**, 312.
23. Hupa, L., Bergman, R., Fröberg, L., Vane-Tempest, S., Hupa, M., Kronberg, T. *et al.*, Chemical resistance and cleanability of glazed surfaces. *Surf. Sci.*, 2005, **584**, 113–118.
24. Kuisma, R., Fröberg, L., Kymäläinen, H.-R., Pesonen-Leinonen, E., Piispanen, M., Melamies, P. *et al.*, Microstructure and cleanability of uncoated and fluoropolymer, zirconia and titania coated ceramic glazed surfaces. *J. Eur. Ceram. Soc.*, 2007, **27**, 101–108.
25. Foster, W. R., The system $NaAlSi_3O_8$–$CaSiO_3$–$NaAlSiO_4$. *J. Geol.*, 1942, **50**, 53–73.
26. Yang, Y. and Prewitt, C. T., On the crystal structure of pseudowollastonite ($CaSiO_3$). *Am. Mineral.*, 1999, **84**, 929–932.
27. Azarov, G. M., Maiorova, E. V., Oborina, M. A. and Belyakov, A. V., Science for ceramics production; wollastonite raw materials and their applications. *Glass Ceram.*, 1995, **52**, 237–240.
28. Vogel, M. B., *Chemical approach to glass. Glass science and technology* (*7th ed.*). Elsevier Science Publishing Company, Amsterdam/Oxford/New York/Tokyo, 1984, ISBN: 0-444-99635-4.
29. Sainamthip, P. and Reed, J. S., Glazes for fast-fired wollastonite wall tile. *Ceram. Bull.*, 1989, **68**, 103–106.
30. Kingery, W. D., Bowen, H. K. and Uhlman, D. R., *Introduction to ceramics* (*2nd ed.*). John Wiley & Sons, New York, 1960, ISBN: 0-471-47860-1.